The Environment of Lyman α Absorbers in the Sightline towards 3C273

S. L. Morris¹, R. J. Weymann Alan Dressler and P. J. McCarthy

The Observatories of the Carnegie Institution of Washington, 813 Santa Barbara St., Pasadena, CA 91101

B. A. Smith

Institute for Astronomy, University of Hawaii, Honolulu, HI 96822

R. J. Terrile

Jet Propulsion Laboratory, Pasadena, CA 91109

R. Giovanelli

Department of Astronomy and National Astronomy and Ionosphere Center², Cornell University, Ithaca, NY 14853

and

M. Irwin

Royal Greenwich Observatory, Madingley Rd, Cambridge CB3 0EZ, UK

ABSTRACT

We present new ground-based data following up on the HST discovery of low-redshift Lyman α absorption in the sight-line to the quasar 3C273. Our goal is to investigate the relationship between the low-column-density absorbers and higher column-density objects such as galaxies or H II regions. Narrow-band filter observations with a coronograph show that there are no H II regions or other strong H α line-emitting gas within a 12 kpc radius of the line-of-sight to the quasar, at the velocities of three of the absorbers. Broad-band imaging in Gunn r shows that there are no dwarf galaxies at Virgo distances with absolute magnitude above $M_B \approx -13.5$ and within a radius of 40 kpc from the line-of-sight to the quasar. Finally, we present fiber spectroscopy of a complete sample of galaxies within a radius of 1°, down to an apparent magnitude of B \approx 19. Analysis of this sample, combined with galaxies within 10 Mpc of the quasar line-of-sight taken from

¹Present Address: Institute of Astronomy, Madingley Rd., Cambridge CB3 0HA, UK

²The National Astronomy and Ionosphere Center is operated by Cornell University under a cooperative agreement with the U.S. National Science Foundation

the literature, shows that the absorbers are definitely not distributed at random with respect to the galaxies, but also that the absorber-galaxy correlation function is not as strong as the galaxy-galaxy correlation function on large scales. We show that our data are consistent with the hypothesis that all galaxies more luminous than $1/10~\rm L^*$ have effective cross-sections (for association with absorbers whose neutral-hydrogen column-density (Log(NH)) is >13.0), of between 0.5 and 1 Mpc. We also show a clear case of a Lyman α absorber which has no galaxy brighter than M_B=-18 within a projected distance of 4.8 Mpc, and discuss the possibility that Lyman α absorbers are destroyed in a rich galaxy environment.

Subject headings: cosmology — interstellar:matter — galaxies:redshifts

1. Introduction

Understanding the origin and evolution of structure in the universe remains one of the most fundamental and active challenges of current astrophysical research. As the evidence in favor of a cosmological origin for the narrow, displaced absorption lines in QSO spectra became overwhelming, it also became clear that both the metal-line systems and the Lyman α systems are invaluable tools for the study of some aspects of this problem. Since ground-based Lyman α studies refer only to redshifts ≥ 1.6 , they complement studies of galaxy clustering properties, the majority of which involve redshifts much less than this. However, precisely because the redshift regimes have been so different and because it has not been at all clear what relation exists between the typical low-columndensity Lyman α absorbers and galaxies, these two approaches have remained disjoint. It was somewhat unexpected, but pleasing, that low-redshift Lyman α absorbers were found in sufficient numbers to enable meaningful studies of the evolution of the Lyman α absorbers and their relation to galaxies (Morris et al. 1991, Bahcall et al. 1991b). This has presented astronomers with the opportunity to join these two lines of investigation.

There are two levels at which such such attempts can be carried out: 1) Purely statistical investigations aimed at comparing the clustering properties of galaxies and Lyman α absorbers, and 2) Investigation of individual cases in which the possibility of establishing the presence (or absence) of a clear link between a Lyman α absorption line and something we could call a "galaxy" presents itself. Preliminary discussions along these lines may be found in papers by Bahcall et al. 1992a, Bahcall et al. 1992b and by Salzer 1992. The present paper is a first attempt to pursue both these approaches along the sightline to 3C273. The remainder of this paper is organized as follows: In \S 2. we describe the different sets of observations we have assembled to investigate the environment of the Lyman α absorbers along the 3C273 sightline. In § 3. we analyze them for possible associations or lack of associations of individual Lyman α absorbers with galaxies, and also give some statistical analysis of the clustering properties of the Lyman α absorbers with galaxies. In § 4. we discuss these results in light of current models for the Lyman α absorbers and provide a brief summary and suggestions for further work.

Throughout this paper H_0 is taken to be 80 km/s/Mpc, the distance to the Virgo cluster is taken to be 16.0 Mpc (a distance modulus of (m-M)_{Virgo}=31.02) (Jacoby *et al.* 1992), and q_0 is taken to be 0.

2. Observations and Reduction

It has long been realized that imaging of the gas directly responsible for the low-column-density Lyman α absorbers is well beyond the reach of current technology. Specifically, the neutral-hydrogen column densities of order $10^{13}-10^{14}~{\rm cm}^{-2}$ that GHRS detected toward 3C273 are about 4 or 5 orders of magnitude below what can be imaged in 21 cm emission, even without taking into account the powerful radio background contributed by 3C273 itself. The H α recombination surface brightness associated with these neutral-hydrogen column-densities is also several orders of magnitude below what is feasible to detect, unless the incident flux of ionizing photons is several orders of magnitude higher than that expected from the integrated background radiation.

However, it has frequently be suggested that the Lyman α absorbers are intimately connected with, or are actual extensions of, entities which can be imaged either by means of $H\alpha$ emission, starlight, or 21 cm emission - e.g. dwarf galaxies (Fransson and Epstein 1982) or shells of expanding gas (Chernomordic and Ozernoy 1983) or the outer regions of galactic disks (Maloney 1992). In the case of dwarf irregulars, for example, a very small episode of recent star formation might betray the presence of a dwarf irregular whose outer envelope produces the Lyman α absorbers. Alternatively, expanding shells of gas might produce $H\alpha$ emission via collisional ionization at a shock front.

In addition, of course, possible association of individual Lyman α absorbers with specific galaxies, as well as statistical studies of absorber-galaxy correlation can be carried out with a sample of redshifts for galaxies in the field surrounding 3C273.

In this section we describe three such new sets of observations of a region centered on 3C273. These are: \S 2.1. Coronagraph observations with narrowband filters of a 5' diameter region, \S 2.2. Deep broadband imaging of a 17' diameter region, and \S 2.3. Fiber spectroscopy of a $2.2\times1.6^{\circ}$ region down to a limiting magnitude of B=19. We describe the analysis of these three sets of observations in \S 3.

2.1. Coronagraph Observations with Narrow Band Filters

Observations of a 5.3 \times 5.3 region (radius \approx 12 kpc at Virgo) around 3C273 were obtained during 1992 February 3-7, with the University of Hawaii Coronagraph (Vilas and Smith 1987) on the Las Campanas 2.5m duPont Telescope. A thinned 1024×1024 Tektronics CCD was used, binned 2×2 , giving a scale of 1.23"/pixel. The coronagraph blocking mask had a diameter of 5". Data were obtained with a Gunn r filter, and also 5 specially acquired filters, 3 with width 13.5Å, centered at 6586.2Å, 6598.0Å and 6756.0Å (hereafter referred to as VN1, VN2 and HN), and 2 with width 25Å, centered at 6643.2Å and 6718.9Å (hereafter referred to as VB and HB). (The above widths and central wavelengths are quoted for an f7.5 beam and a temperature of 15° C). The narrow-band wavelengths were chosen to match the redshifted position of H α at the velocities of the 2 Lyman α absorbers listed in Morris et al. 1991 at velocities corresponding to the Virgo cluster (Bingelli, Sandage and Tammann 1985), and one absorber at 1251Å. This is the lowest redshift, strong Lyman α system beyond the Virgo cluster. The observing procedure involved cycling through the 6 different filters, with exposure times of 10 mins for the r and 25Å filters, and 20 mins for the 13.5Å filters. Seven such cycles were completed over the 5 night run. During the observing run, it was discovered that the narrow-band filter HN had slightly non-parallel faces, resulting in detectable 'ghost' images offset from bright stars and also 3C273. In an attempt to minimise the effect of these, this filter was rotated though 90° between each night.

For calibration purposes, observations were also obtained of Mkn 49 (an emission line galaxy in the Virgo cluster with radial velocity 1524 km/s, and hence with H α line-emission within 2Å of the peak of VN2) and M87, and also a number of bright standard stars.

The images were reduced using IRAF³. The reduction steps were: bias subtraction, division by a flat field taken on the same night as the observations, rotation and shifting of the images to match a reference image, sky subtraction and averaging together of images taken with the same filter. It was found after the run that refocusing the coronagraph between taking the flat fields and the data meant that the flat field di-

vision left significant features in the data, both at the edges of the coronagraph field and also throughout the data at the location of what are presumed to be dust particles on the coronagraph optics or CCD window. This problem was particularly noticeable for the data taken on the last night of the run. However, the residuals are greatly reduced in the combined data.

Continuum sources were removed from the narrowband images by subtracting off a scaled version of the two 25Å filter observations. We investigated scaling methods, including measuring stars or galaxies in the images, but found that the scaling derived was consistent with simply subtracting off the average of the 25Å filters from each 13.5Å observation. That is, there was no evidence for a significant continuum slope or calibration difference across the 150Å region of interest, and the factor 2 shorter broad-band exposure fairly accurately balanced the higher throughput of the 25Å filters. This apparent consistency may be fortuitous: due to the small field (small number of galaxies), and the errors in measuring the flux of faint galaxies. Figure 1 shows the sum of the 25Å data, and the continuum subtracted 13.5Å data for 3C273. As can be seen, the PSF is a function of angle off-axis, and becomes quite broad and asymmetric at the edge of the field, due to aberrations in the coronagraph optics.

2.2. Wide Field Imaging with COSMIC

A mosaic of Gunn r band images of the field around 3C273 was obtained on 1992 February 23, at the Palomar 5m, with the prime focus COSMIC system. This recently commissioned camera contains a thinned 2048×2048 Tektronics CCD. Due to poor seeing, this was read out with 2×2 binning giving a scale of 0.56"/pixel. Exposures were taken roughly centered on 4 positions offset from 3C273 by 5'.4 NE, NW, SE and SW. Four exposures of 5 minutes each were obtained at each position. During the observations, the moon rose, and so the background level of the images varies by almost a factor 2.

The data were reduced using IRAF. After bias subtraction, the data were flat fielded using images of the dome. This left significant large scale structure in the images, and so a 'skyflat' was constructed from the combined data images. This flat was median smoothed to remove any small scale structure. Because of a region of very low sensitivity near the center of the CCD, and also the location of a very bright star coincidentally at the same place in one set

 $^{^3\}mathrm{IRAF}$ is distributed by NOAO, which is operated by AURA Inc. under contract to the NSF

of images, the flat fielded data still shows a weak negative feature near the center of each image. The sky background was determined for each image separately and subtracted. The offsets between the images were determined by measuring the positions of the QSO and 2 bright nearby stars, which were common to all images and the data were then mosaiced together, giving a combined image with diameter 17.2 centered on 3C273. The resulting image is show as figure 2.

2.3. Fiber Spectroscopy

During 1992 February 8-10, spectra of objects in a $2.2\times1.6^{\circ}$ rectangle surrounding 3C273 were obtained with the Fiber Spectrograph at the Las Campanas 2.5m duPont Telescope. (Shectman 1992). This system has 128 fibers which are manually plugged into an aluminum plate over a $1.5\times1.5^{\circ}$ field. The fibers have a projected diameter of 3".5. They feed the slit of a floor-mounted spectrograph. A 600 l/mm grating was used, with the 2D-Frutti photon-counting detector, giving a resolution of 8.6Å FWHM. Three fields were observed for about 6000 seconds each, offset EW from each other.

Objects observed were chosen from a database produced by scanning an UKST IIIaJ plate of the region with the APM scanning machine at Cambridge. The APM produces a catalog of all the objects on a plate, with estimates of isophotal magnitudes, size and a 'sigma' parameter that measures how much the image parameters differ from those of stars with comparable magnitude. We chose objects to observe from this catalog with 'sigma'>3.0. This includes many fairly compact objects, and resulted in a rather high contamination by stars, but also means that we found a number of compact galaxies that would otherwise have been missed. For each 1.5×1.5° fiber field, a magnitude sorted list of candidate galaxies was produced. Due to restrictions on the minimum fiber separation, 330 out of a possible 336 object fibers were used, with 16 fibers per field set on blank sky.

The fiber spectra were extracted and reduced using the IRAF apextract package. The spectra were first traced and extracted. Then fiber-to-fiber throughput differences were corrected with a flat field image, and the fibers were wavelength calibrated and rebinned to a common linear wavelength scale. The wavelength calibration used an arc spectrum to determine the non-linear relationship between wavelength and pixel number, after which a zero point shift was measured for each fiber using the strong sky lines in the data.

Finally, the sky emission was subtracted from each fiber using an unscaled template constructed from the 16 sky fibers in each frame.

Classification and radial velocity measurements for each spectrum were done in two ways. First each spectrum was inspected by eye, and classified as either a star, galaxy or unknown. Then a radial velocity was determined by measuring either the position of the 4000Å break, or that of the [OII] $\lambda 3727.6$ feature (actually a doublet, but unresolved in our data). A subjective assessment was also made of the reliability of the resulting radial velocity, dividing the sample into 'possible' and 'definite'. All the spectra were also analysed using the fxcor routine in IRAF. Each object was cross-correlated with three different templates: (a) a template made up from the 27 best S/N stars in the data, (b) a template made up from 3 high S/N late-type stars, and (c) a template made up from 16 emission line galaxies (all shifted to their rest frames) in the data. For each spectrum, the correlation with the highest peak was then selected. A reassuringly close match was found between the by-eye classification and velocities and the results from fxcor. The resulting histogram of velocities was inspected. Apart from 4 low S/N or hot stars (for which a good template was not constructed), the stellar velocities found by fxcor had a distribution well represented by a gaussian with zero mean and an approximate dispersion (σ) of 85 km/s. We take this to be a reasonable estimate for our radial velocity uncertainties. It was also found that the subjective 'possible' category in the by-eye radial velocity measurements matched rather well to a cross-correlation peak height less than 0.3 returned by fxcor. Apart from one outlier, the difference between the fxcor velocity and that measured by eye for the galaxy identifications with crosscorrelation peak heights above 0.3 also was fairly well fit by a gaussian with σ of 85 km/s.

In the end we obtained 129 definite galaxies, 43 possible galaxies, 86 definite stars, 4 possible stars, 10 fibers that had to be unplugged due to overillumination (which were hence almost certainly stars), 37 fibers which showed no flux (either very low surface brightness galaxies or positional errors) and 21 spectra which showed flux but which were unclassifiable either as stars or galaxies (based on very low cross-correlation peak heights from fxcor and visual inspection). We should reiterate that a much higher 'success' rate in finding galaxies could have been achieved by raising the cutoff 'sigma' value used in choosing

galaxies from the APM scans, at the cost of missing some compact galaxies.

We present in table 1 the resulting galaxy redshifts. For each object, the table lists the RA and Dec, an approximate B magnitude and the heliocentric radial velocity. The magnitudes were calculated using the APM isophotal magnitudes measured from the plates, crudely calibrated using the B magnitudes listed by Stockton 1980 and Salzer 1992 for objects in the scanned region. They could be in error by as much as 0.5.

A number of the brightest galaxies in the field were not included in the fiber survey. Those with known redshifts within the survey region were added to the sample (4 objects taken from the May 5 1990 version of the CfA Redshift Catalog, Huchra 1990). This gives a total sample of 176 galaxies with redshifts within the survey region which is roughly complete to a B magnitude of 19.0.

We plot the results of the survey in a number of projections. Figure 3 shows a redshift histogram of the galaxies, figure 4 shows the distribution of galaxies on the sky, while figure 5 shows the pie-diagrams obtained.

3. Analysis

In this section we go through each of the three observations described in \S 2. in turn, deriving constraints on the absorbers. In \S 3.1. we derive limits on H α line emission at the velocities of the narrow-band filters and in \S 3.2. we calculate the maximum absolute magnitude a dwarf galaxy could have and remain undetected in our broad-band imaging. A long description of the correlation analysis between the Ly α absorbers and the galaxies found in the fiber survey is given in \S 3.3., in which the various available absorber and galaxy sub-samples are discussed, and two alternative extreme hypotheses for the absorber-galaxy correlation function are tested. Finally in \S 3.4. we discuss some particular aspects of the absorber-galaxy distribution found in the 3C273 sightline.

3.1. Flux Limits for $H\alpha$ Line Emission

The final continuum-subtracted coronagraph images have a measured rms dispersion (away from residuals due to bright stars) of 0.0018 DN/pixel/s. From calibration observations of HD84937, this is equivalent to a 1σ flux limit of 2.10^{-18} ergs/cm²/s/ \square ", equivalent to an emission measure of approximately

2.8 pc cm⁻⁶. By blinking the images, it can be seen that none of the objects visible in the broad-band images have emission line fluxes $> 3\sigma$. For comparison, the VN2 image of Mkn49 showed a peak H α line flux of 3.10^{-14} ergs/cm²/s/ \square ", i.e. 5,000 times higher than our 3σ detection limit. One can also perform the following thought experiment. What would the Orion nebula look like if placed at the distance of the Virgo cluster? As discussed in Kennicutt 1984, the Orion nebula is actually a relatively low luminosity H II region, with an H α luminosity of only 10^{37} ergs/s. Nevertheless, if placed at a distance of 16 Mpc, it would still have a flux of $1.3 \ 10^{-15} \ ergs/cm^2/s$ (and would be unresolved - the nebula has a diameter of 5 pc, while at Virgo, 1" corresponds to approximately 80 pc). Thus it would be a factor 220 brighter than our 3σ limit. One can also calculate that the Stromgren sphere around a single main sequence star of spectral class $\sim B1/\square''$ would be detectable at the 3σ level (Allen 1973).

Unfortunately, the expected surface brightness of an optically thick slab of hydrogen, simply bathed in the local UV background would not be detectable. Taking the limit on the UV background from Songaila, Bryant and Cowie 1989, and using the formulae from Osterbrock 1989, one finds a surface brightness of $\leq 3.10^{-19} \ {\rm ergs/cm^2/s/\square''}$, about a factor 20 below our 3σ limit.

Higher spectral and spatial resolution data have been taken by T. Williams (private communication) using the Rutgers Fabry-Perot system at the CTIO 4m telescope. This data has not been fully analysed, but should produce even lower surface brightness limits (or detection) than our data.

3.2. Limiting Magnitude for detection of Low Surface Brightness Dwarf Galaxies

The main motivation for taking the COSMIC images was to determine whether there were any dwarf galaxies within a 40 kpc radius from the line of sight to 3C273 which are too faint to be visible on the POSS sky survey plates. Examples of low surface brightness dwarfs in the Virgo cluster can be seen in Sandage and Bingelli 1984. In order to determine how faint a dwarf galaxy, which had morphological properties typical of those found in the Virgo cluster, would be detectable in our image, we used the IRAF artdata package to insert artificial dwarf galaxies into the data array. The magnitude scale was derived by assuming that the sky background in the Gunn r band (before

the moon rose) was 21.5 (Massey 1990). B absolute magnitudes were converted to Gunn r assuming a B-R color of 1.0 (B-V of 0.7), and a conversion from R to Gunn r of r=R+0.43+0.15(B-V) (Kent 1985). Thus a dwarf galaxy with $M_B=-15.5$ was taken to have $M_r=-15.5$ 16.0. The Virgo distance modulus was taken to be 31.02. Dwarf galaxy properties were taken from Bingelli, Sandage and Tammann 1985. In particular, typical exponential scale lengths⁴ for Virgo dwarfs were taken to be 2-4 kpc. Figure 6 shows the same data as figure 2, but with three dwarf galaxies added. One to the NE with M_B =-14.5 and scale length 4.4 kpc, one to the NW with M_B =-13.5 and scale length 2.2 kpc, and one to the SW with M_B =-13.5 and scale length 4.4 kpc. These experiments demonstrated that we would be able to detect dwarf galaxies as faint as -13.5 at the distance of Virgo, having morphological properties similar to those found near the cluster center. For comparison, the dwarf galaxy illustrated in figure 2, panel 4, labelled '15°47' of Sandage and Bingelli 1984 has an absolute B magnitude of -14.8.

A complementary approach is to search for H I 21 cm emission from Virgo dwarf galaxies. Recently, van Gorkom and her collaborators have set extremely low limits with the VLA over a 40×40 arcmin field centered on 3C273 and over a velocity range of about 1000 km/s centered on 1300 km/s to a 1 sigma column-density limit of approximately 10^{19} cm⁻² (van Gorkom 1993, van Gorkom $et\ al.\ 1993$).

3.3. Correlations between Lyman α Absorbers and Galaxies

We have shown there are no H II regions, or other strong $H\alpha$ line-emitting gas, or dwarf galaxies near the Virgo absorbers. Having determined the redshift distribution of galaxies near the sightline to 3C273, (§ 2.3.) we would now like to address the statistical question of the degree to which the Lyman α absorbers are correlated with luminous galaxies. If they are correlated, is the Lyman α absorber-galaxy correlation the same as the galaxy-galaxy correlation? A cursory inspection of figure 5 is enough to show that there will not be a simple answer to this question. While there do seem to be Lyman α absorbers associated with clumps of galaxies (e.g. the Virgo absorbers, or the set of absorbers around z=0.02-0.03), there are also absorbers in conspicuous 'voids' (at z=0.06-0.07), and there are no absorbers associated with the prominent excess of galaxies at z=0.078. We consider statistical tests for various assumptions about the correlation between the Lyman α absorbers and the galaxies near the sightline towards 3C273 for which we have redshift information. Ultimately, the goal should be a quantitative and complete statistical description of the clustering properties of the Lyman α absorbers themselves and their correlation with various types of galaxies, clusters, voids etc. Given both our rather meagre understanding of this problem and the small data set, we shall concentrate on testing the following two extreme null hypotheses about the Lyman α absorber clustering properties:

- 1. The Lyman α absorbers are uncorrelated with galaxies and are randomly distributed. (The second part of this assumption necessarily implies the first, but the converse is not necessarily true: The absorbers could be correlated among themselves but be uncorrelated with galaxies)
- 2. The Lyman α absorbers are correlated with galaxies in the same way that galaxies are correlated. More precise formulations of this hypothesis depend upon the particular test applied, as described below.

In carrying out most of the tests described below, it is necessary to compute the 3-dimensional distance between every absorber-galaxy or every galaxy-galaxy pair. The question arises as to how to compute the component along the line of sight, since departures from a perfectly smooth Hubble flow distort the mapping of redshift onto radial distance. With no information other than the angular coordinates and redshifts for the objects, we cannot uniquely determine the separation along the line of sight for any individual pair of objects. For purposes of statistical tests we therefore make two different assumptions about this component; the degree to which we do or do not derive similar results will provide some indication of the sensitivity of the test to the uncertainty in the estimation of this component:

- 1. We simply ignore any departures from Hubble flow
- 2. We adopt the formalism of Davis and Peebles 1983 to estimate this component. These authors show how, knowing the two-point correlation function for the *projected* distance between

⁴Scale Length= R_0 , with Intensity $\propto \exp(-1.6783 \times R/R_0)$

pairs, in principal one can invert the integral equation relating the projected distance correlation function to the three-dimensional spatial correlation function. However, for our limited and rather noisy sample, this is not a very satisfactory procedure. Moreover, we would like statistical estimates for the 3-dimensional separation for each pair for the purposes of carrying out other types of tests (e.g. nearest neighbor tests). We therefore use the Davis-Peebles formalism as follows: Adopting the assumptions described in their paper, the integrand in their equation (22) represents the probability that a pair with projected separation r_n Mpc and velocity difference π km/s has a separation in the radial direction of y Mpc. We further assume their functional form for h(r) in their equation (23), with the parameter F = 1, and adopt their functional form for f(V), the probability of the relative velocity difference, as well as their expression for σ , the dispersion in f(V), i.e. their equation (32). For $r_p >> r_o$ or $\pi >> H_o \times r_o$, where r_o is the characteristic correlation length, the probability is strongly peaked at $y \sim H_o \times \pi$, i.e., the pair separation is very likely to be that given by assuming a pure Hubble flow. However, as both of these inequalities fail to be satis fied, a second maximum in the probability distribution arises at $y \approx 0$ whose height depends upon the strength of the correlation - i.e., a pair with a moderate velocity separation and small projected separation may be separated by their Hubble flow distance, but if the correlation between such pairs is strong, this moderate velocity separation is more likely to arise from a pair at about the same distance from us, with strong gravitational interaction between them. As noted at the outset of this discussion there is no way to unambiguously determine the relative separation of any pair along the line of sight, but since we are interested in statistical applications we adopt the expectation value of this probability distribution as our second alternative algorithm.

A problem with this second approach is that evaluating the probability distribution for the radial separation of the pair requires that we know in advance the two-point correlation function between the pair. Ideally, we could have dealt with this problem by using an iterative approach: for both the absorber-

galaxy and galaxy-galaxy pairs separately, we start with some "fiducial estimates" for the two-point correlation (e.g. $r_o = 5.4h^{-1}$ Mpc and $\gamma = 1.77$; c.f. equation 19 in Davis and Peebles) to compute the expectation value of the radial separation for each pair, and thus compute the two-point correlation functions. With these new, separate best-fit values of γ and r_o for the correlation functions for the galaxy-absorber pairs and the galaxy-galaxy pairs, we could then repeat the process until the parameters for the twopoint correlation functions have converged. In fact, since the results of our statistical tests do not appear to be very sensitive to departures from a pure Hubble flow, we have not carried out this iteration, but have simply used the single set of parameters $(r_o = 5.4h^{-1})$ Mpc and $\gamma = 1.77$) in calculating the expectation values for both sets of pairs.

In the following, we refer to these two algorithms for estimating the radial separations as the "pure Hubble flow" and "perturbed Hubble flow" cases. When listing object separations in the following sections we will give the separations found from the expectation value of the perturbed Hubble flow model in brackets following the value for the pure Hubble flow model.

Before carrying out any statistical tests we define the two samples and discuss appropriate corrections for completeness.

3.3.1. The Lyman α Sample

A carefully defined list of Lyman α absorption lines is essential to a proper statistical discussion of the correlation properties of Lyman α absorbers with galaxies. The preferred list would obviously be drawn from a homogenous set of observations with the smallest detectable equivalent width covering all or most of the relevant redshift range.

Several line lists for the 3C273 sight line have been published (Morris et al. 1991, Bahcall et al. 1991a, Bahcall et al. 1991b, Brandt et al. 1993, Bahcall et al. 1993). These line lists are compared in table 2. However, not only are these lists based upon 3 different HST spectrograph configurations (GHRS G160M, GHRS G140L, FOS G130) but they have also been produced by different reduction procedures and line-finding and measuring algorithms and with differing acceptance criteria for what constitutes a "real" line. To investigate the importance of this latter source of inhomogeneity we have run the same

continuum fitting, absorption line-finding and linemeasuring software, "JASON", used for the FOS line list, which is described in detail by Schneider et al. 1993^5 on the data sets of Morris et al. 1991 and Brandt et al. 1993. The JASON software was designed to run on FOS data with an approximately gaussian point spread function (PSF). Unfortunately this is not a good representation for the GHRS large aperture PSF, and also in general the lines were resolved - meaning that the observed line profiles had neither the instrumental PSF nor a gaussian shape. The current version of JASON does not perform such convolutions, and so we have run the search routines assuming a fixed PSF with the correct (non-gaussian) shape for the GHRS, but with no account taken for resolved lines. This means that the EWs output by the JASON software are not accurate, but the detection significance levels are approximately correct (see Schneider et al. 1993). The data set used is that described by Brandt et al. 1993. We tabulate the significance levels from JASON for the Lyman α lines in column 5 of table 2, after the positions and EWs published in Brandt et al. 1993. It can be seen that all of the 'reliable' lines listed by Morris et al. 1991 are confirmed by the JASON software, with the notable exception of the line at $\lambda 1276.54$, which was also not found by Brandt et al. 1993. We checked this line by running the JASON software on the original data used by Morris et al. 1991, obtaining a significance level of 4.5 for the line. The line finding and fitting software used in Morris et al. 1991 was developed by R. Carswell and J. Webb, and is described in that paper. It used the GHRS PSF convolved with a Voit profile with variable width.

Two other entries in table 2 require special comment: The line at $\lambda=1317.08$ is identified as Lyman α in the list of Bahcall et~al.~1991b whereas in the list of Morris et~al.~1991 it is identified as Ni II. This issue has been discussed in detail in Brandt et~al.~1993 who give reasons for preferring the Ni II identification which we adopt. The second case involves the line at $\lambda=1393.86$. As discussed in detail by Savage et~al.~1993 this line appears to be a blend of one of the members of the galactic Si IV doublet and another strong line, whose only plausible indentification is Lyman α . The procedure used by Morris et~al.~1991 in estimating the strength of this line (which in-

volves a detailed comparison of the line profiles of the Si IV doublet) is not incorporated into the JASON formalism. For this reason we cannot assign a formal uncertainty in the line strength. However the residuals from an unblended fit to the Si IV doublet are highly significant.

As a result of the above considerations, we have decided to adopt the following samples of absorbers for our statistical tests: (1) For the Lyman α absorber "full sample" we adopt the list of 16 Lyman α absorbers (and their redshifts) given in Morris et al. 1991 along with the additional low-redshift line $(\lambda 1224.52)$ given by Bahcall et al. 1991a; as noted in table 2, this last line is visible in the GHRS G140L spectra but was below the significance threshold of Morris et al. 1991. This "full sample" is inhomogenous and/or biased in three senses: i) The high resolution GHRS data covers only redshifts above $z\sim0.016$; below this, only the FOS data of Bahcall et al. 1991b and the GHRS G140L low resolution data are available. (Observations with the GHRS G160M grating in the redshift regime from 0.0 to 0.016 are scheduled for HST Cycle 3). Thus, the full sample may be biased against weak low-redshift lines in this redshift range that may be detected by these Cycle 3 observations. ii) The line of sight toward 3C273 may be somewhat atypical in that it passes through the southern extension of the Virgo cluster. iii) Some of the weakest lines listed as "possible" in the Morris et al. 1991 list may not be real. Accordingly, along with the full sample of 17 lines, we shall also consider two subsamples: (2) A "homogeneous sample" made of the set of 14 lines found only with the GHRS G160M observations using the original Carswell and Webb software (i.e. all but the first 3 lines in column 1 of table 2). (As it happens, this is also equivalent to deleting the 3 low-redshift ($z \le 0.016$) lines possibly associated with the Virgo cluster). (3) A "strong sample" composed of the set of 10 lines from Morris et al. 1991 with $-\log(P) > 7.5$ (but including the line at z=0.14658 for which a formal probability estimate was not possible due to blending - i.e. the above sample with the lines marked 'd' in the comments column of table 2 removed). We have listed the sample membership in the final column of table 2. Note that in contrast to the galaxy sample discussed below there is no intrinsic observational selection against the higher redshift absorbers.

One could, of course, define further samples. In particular, at the request of the referee, we have also

⁵We thank D. Schneider for kindly making available the most recent version of JASON and for instruction in its use.

run our statistical tests of the complete set of 5 lines listed in Bahcall et al. 1993 (i.e. the line list in column 8 of table 2). Unfortunately, the number of lines in this list is so small that neither of the two null hypotheses considered below in connection with cloud-galaxy association can be rejected with any significance. For this reason, and in order to keep the various combinations of absorption line and galaxy samples to managable proportions, we limit our tables of statistical results to consideration of the three samples defined above.

3.3.2. The Galaxy Sample

An appropriate sample of galaxies with which to carry out the correlation analysis would be one which is complete to some limiting absolute magnitude throughout a cylindrical volume centered on the 3C273 sightline (i.e. out to a constant impact parameter) with a radius large enough to sample most of the expected power in the correlation function and length over (and beyond) the full redshift range covered by the Lyman α line sample. The observed sample described in $\S 2.3$. fails this requirement in two obvious respects: i) It detects only the more luminous galaxies at the higher redshifts, ii) It contains no galaxies with large impact parameters at low-redshifts. For some tests these deficiencies are probably not important but for others they are. Accordingly, we will consider two galaxy samples. The first is the sample described in § 2.3., which we will refer to as the 'cone' sample. The second is the cone sample together with all galaxies from the May 5 1990 version of the CfA Redshift Catalog, (Huchra 1990) within 10 Mpc of the 3C273 lineof-sight. This gives a heterogeneous sample with an unknown selection function, but is closer to the ideal 'filled cylinder' than the cone sample. It contains 1498 galaxies, the vast majority being at Virgo distances, and will be referred to as the 'cylinder' sample.

Thus for each hypothesis tested below there are 6 galaxy-absorber sample combinations, and 2 possible estimates for the distance between every pair of objects giving a total of 12 data sets for each statistical test.

3.3.3. Tests of the 1st Null Hypothesis: The Lyman α absorbers are uncorrelated with galaxies

It is obvious that this hypothesis cannot literally be true - every sightline that passes close to any galaxy, except those utterly devoid of gas, will surely produce a detectable Lyman α line, and indeed examples of this are already known (Bahcall *et al.* 1992a, Bahcall *et al.* 1992b). Nevertheless, in light of the fact that the high-redshift Lyman α absorbers show almost no power in their two-point correlation function (c.f. Rauch *et al.* 1992 and references therein) it is of interest to see if the present data set does or does not exclude this hypothesis, and if it does, how strongly.

Having formulated this null hypothesis we consider two statistics as measures of correlation (or lack of it):

- 1. The average over all the Lyman α absorbers of the distance between a given Lyman α absorber and the N nearest galaxies in the sample, with N=1,3 and 5.
- 2. The total number of absorber-galaxy pairs within a fixed radius R, with R=500 kpc and 10 Mpc.

In order to see whether the values of these observed statistics are such that the null hypothesis can be rejected, we must find the distribution of these same statistics for many realizations of the null hypothesis. To do this, we carry out 1000 Monte Carlo simulations in which the same number of absorbers as that of the particular Lyman α sample under consideration are laid down randomly (but follow the "global" distribution $dN/dz \sim (1+z)^{0.3}$ as determined by Bahcall et~al.~1993). Redshift limits for the random absorbers were 0.03 < z < 0.151 for the total sample, and 0.016 < z < 0.151 for the homogeneous and strong samples.

The results for the nearest-neighbour tests are summarised in table 3. We show results for the single nearest neighbour galaxy, the mean of the 3 nearest and the mean of the 5 nearest. For each case, the three columns list the observed mean nearest-neighbour(s) distance, the average of the mean nearest-neighbour(s) distances produced by the Monte Carlo simulations, and the number of the 1000 Monte Carlo simulations that had a mean nearest-neighbour distance less than the observed one. Thus this last column, divided by 1000, can be taken as the probability that the observed value could arise from a sample of absorbers distributed at random with respect to the galaxies.

The most striking result is that there is a less than 0.1% probability that the average nearest-neighbour distance to the single closest galaxy could arise from a randomly distributed set of absorbers. This is true for all sample combinations, and for either pure or

perturbed Hubble flow. For all samples, as one includes more galaxies in the nearest-neighbour average, the significance drops. After seeing this result, we wanted to test whether all the significance came from the nearest galaxy, and so ran tests on the second nearest galaxy only (also given in table 3). One can see that the observed mean distance is still significantly lower than that expected for a randomly distributed set of absorbers, but this could be explained by a combination of the highly significant correlation with the nearest galaxy and the strong galaxy-galaxy two-point correlation. This point is discussed in some detail by Phillips, Disney and Davies 1993 in the context of bright galaxies found near quasar MgII absorbers.

We also give in table 4 the RA, Dec and redshift of the nearest galaxy in the 'cylinder' sample to each Ly α absorbers of the 'total' sample (assuming pure Hubble flow). The final column in this table is the minimum absolute magnitude that could have been detected in the fiber survey. This shows that for one absorber there is no known galaxy with absolute magnitude above -17.8 within nearly 10 Mpc, (the same distance for the perturbed Hubble flow model) and that even the nearest absorber-galaxy pair in our sample are separated by 350 kpc (240 kpc). We will return to this in § 3.4.

The results for the number of galaxies within a fixed radius of each absorber are given in table 5. These tests are essentially a comparison of the integrated two-point correlation function out to the given radius (see Mo et al. 1992 for a discussion of this point). The numbers given in the table are the observed number of absorber-galaxy pairs within the given radius, the average of the number of pairs found in 1000 Monte Carlo simulations with randomly distributed absorbers, and the number of the Monte Carlo simulations with a larger number of pairs than that observed. Thus the final column divided by 1000 is the probability that the observed numbers of pairs or more would arise from a random distribution of absorbers.

Table 5 shows that there is no significant excess of galaxies within volumes of radius 10 Mpc centered on the absorbers compared to a random distribution, apart from the cylinder/total subsample. For this combination there are a large number of pairs between the Virgo absorbers and the many Virgo galaxies in the CfA catalog. This result may be interpreted as saying that it is surprising to find 3 out of 17 absorbers

below z=0.008 (although see § 3.4.3.). There is a marginally significant excess of absorber-galaxy pairs within 500 kpc, over that expected for a random distribution of absorbers, although the inclusion of the Virgo velocity range removes the significance of this result. In summary, these tests seem to be consistent with the nearest-neighbour distance results, showing that there is an excess of close pairs of absorbers and galaxies, but that this result vanishes if the averaging is done over several galaxies or large radii.

3.3.4. Tests of the 2nd Null Hypothesis: Identical Lyman α absorber-Galaxy, Galaxy-Galaxy Correlations

In order to test this hypothesis, one would like to use the same tests as were used in § 3.3.3. A difficulty arises though in generating a large number of Monte Carlo samples. We are loathe to compare the observed distributions with simulations involving anything other than the actual observed galaxy distribution since differences between the observations and simulations (based, for example on n-body or other galaxy clustering models) may result simply from inadequacies of such models, and it is not clear how to create simulations of (fake) absorber-(real) galaxy distributions having cross correlation properties which are the same as the observed galaxy-galaxy correlation properties.

One way to deal with this difficulty is to use a test which does not require the generation of Monte Carlo samples: If the absorbers are distributed in the same way as the galaxies, then, given the pencil-beam nature of the galaxy sample, the redshift distributions of the absorbers and the galaxies should be identical, after correction for differing selection effects in the two samples. Table 6 shows the Kolmogorov-Smirnov D-values and probabilities that the absorber redshift distribution is the same as that of the galaxies, after the galaxy distribution is corrected using the selection function shown in figure 3. This selection function was derived by assuming a Schechter luminosity function with $M_*=-19.5$ and $\alpha=-0.97$ (Loveday et al. 1992). Because this test requires a known selection function, it can only be run for the 'cone' galaxy sample. Also, as it directly compares the redshifts, it does not require any assumptions about pure or perturbed Hubble flow. It can be seen from table 6 that when all the absorption lines are included there is a highly significant difference in the redshift distributions. This significance level becomes marginal when the Virgo absorbers are removed, and vanishes when only strong absorbers beyond Virgo are considered.

Our other test of the hypothesis that the absorbers and galaxies have identical correlation functions uses the observed galaxy sample to generate our Monte Carlo 'absorber' sample. For each realization a number of the actual galaxy redshifts were selected at random, and were treated as absorbers on the 3C273 sightline. The actual algorithm involved selecting at random a number of the observed galaxy redshifts equal to the number in the absorber sample (making no correction for the galaxy selection function, and with no restriction on how close together the chosen galaxies were), and treating these redshifts as if they were measured absorber redshifts on the 3C273 line of sight. The galaxies which provided these redshifts were removed from the galaxy sample for each test, to avoid an excess of 'spurious' pairs⁶. The number of absorber-galaxy pairs within a given radius were determined for both the real and 1000 Monte Carlo samples, in an identical manner to the second test in $\S 3.3.3$. above. This procedure should be valid as long as the radius within which the pair counts are being made is significantly larger than the typical distance between a galaxy and the 3C273 line-of-sight. Because of this, tests were not run for a 500 kpc radius. The results from these tests are given in table 7. The columns are the same as for table 5, except that the final column lists the number of Monte Carlo runs with fewer absorber-galaxy pairs than the real sample. Thus this number divided by 1000 is the probability that the absorbers could have a correlation function as strong as that between galaxies. As can be seen, the absorber-galaxy correlation function averaged over 10 Mpc is significantly weaker than that between galaxies.

In summary, the two tests above seem to show that the absorber-galaxy correlation function is significantly weaker than the galaxy-galaxy correlation function over large scales (10 Mpc). Even though there is clear evidence for galaxy-absorber clustering, there is a significant difference between the strength with which the galaxies are clustered with respect to each other and the strength with which the Lyman α

absorbers are associated with galaxies.

Some of the results of the two preceding sections can be inferred directly by inspection of the actual two-point correlation functions themselves. A logarithmically binned version of the correlation functions for pure and perturbed Hubble flows are shown in figure 7. The absorber-galaxy correlation function was generated using the total Lyman α sample and the cone galaxy sample. The correlation functions were normalised in the usual way using random samples with the selection function shown in figure 3. The error bars were estimated using the formulae in Mo, Jing and Borner 1992. As expected, the pure and perturbed Hubble flow models agree fairly well for separations larger than one or two Mpc; the perturbed Hubble flow model produces more very close pairs, since even small velocity differences wipe out small separations for the pure Hubble flow model. In both cases, the absorber-galaxy correlation is clearly weaker than the galaxy-galaxy correlation on scales from about 1-10 Mpc. However, although visual inspection of the absorber-galaxy correlation function may suggest that the correlation is significant out to about 10 Mpc, in fact the pair tests summarized in table 5 and the nearest neighbor tests summarized in table 3 both indicate that a statistically significant absorber-galaxy correlations can be detected in our data sets only over volumes which are smaller than this.

3.4. Some Particular Cases of Interest

3.4.1. The Closest Absorber-Galaxy Associations

Actual associations between individual observed galaxies and absorbers in the 3C273 sight line are difficult to prove for a number of reasons: (1) The smallest projected distance to the 3C273 line-of-sight of all the galaxies in our sample is still 160 kpc. (2) Galaxy rotation or velocity dispersions could produce velocity differences as large as 200 km/s between the mean galaxy velocity and an actually associated absorber (also comparable to the 3σ error in our fiber data velocity measurements) (3) In regions of high galaxy density along the line-of-sight, peculiar motions of the galaxies and the absorbers in cluster potential wells may make the velocity-distance relationship complex. This is especially true of the Virgo region, and for the z=0.0034 and 0.0053 absorbers (which also lie on the steep portion of the damping wings of the galactic Lyman α , and have only been observed at low resolu-

⁶In fact leaving in the galaxies would allow one to model a situation where the absorbers were actually part of the halo of one of the observed galaxies, although some maximum halo size would also have to be imposed to make the simulation realistic. We are investigating this point in more detail, and a paper is in preparation (Mo, Morris and Weymann 1993)

tion). With these caveats, it can be seen from table 4 that the closest absorber-galaxy pair has a separation of 350 kpc (240 kpc). Outside of the Virgo region (where the velocity-distance relationship may be less complex, but also where our galaxy sample goes to much less faint absolute magnitudes), the smallest separation is 410 kpc (350 kpc).

The best published example of an association between a Lyman α absorber and a galaxy is given in Bahcall et al. 1992a, where they find a galaxy within 90 kpc of the sightline to H1821+643 which has a strong Lyman α absorber (EW 950 mÅ) within 400 km/s. There are no galaxies in our sample this close to the line of sight (or indeed any absorption systems this strong).

One can (somewhat arbitrarily) break the absorbers in our sample into two groups: (1) those with a galaxy within 1 Mpc of the line-of sight, and with a velocity difference of less than 400 km/s (all of the Virgo systems and 6 of the higher-redshift systems. Despite its entry in table 4, the absorber at z=0.02622 actually has 2 galaxies within 400 km/s and 1 Mpc projected separation. They do not appear in the table, as their large velocity differences (>250 km/s) make their separation large, assuming pure Hubble flow), and (2) the rest (8 systems). There is no significant difference in the EW distribution of these two samples.

Our data can also be used to consider the question: What is the average galaxy diameter within which one would see a neutral-hydrogen column density of at least 10¹³ cm⁻²? In practice this is rather a naive question, as the cross-section almost certainly depends on galaxy luminosity and probably also morphology. One might also expect a patchy distribution of neutral-hydrogen in the outer parts of galaxies leading to a covering factor not equal to one. Nevertheless, ignoring these complications, and excluding the Virgo velocity range due to (a) the possibility of large peculiar velocities (b) a wish to avoid the large range of intrinsic galaxy luminosities in the sample and (c) because our absorber EW limit is higher in this region, we find that of the 12 galaxies with projected separation to the line-of-sight less than 1 Mpc, 8 show Lyman absorption systems within 400 km/s. A velocity difference of up to about 400 km/s could possibly be attributed to internal motions within a large galaxy, coupled with our measuring error, or alternatively to a small group. Having 8 or more such matches would occur 0.6% of the time if the absorbers were randomly distributed in velocity space. However, of these 8 galaxies, two are associated with the absorber at z=0.02622, and three with the absorber at z=0.2933. Clearly several distinct galaxies can not be producing the same absorber, and so in fact only 5 of the 12 systems within 1 Mpc of the line-of-sight to the quasar can be legitimately associated with individual absorbers. Reducing the projected separation to 500 kpc, one finds 3 galaxies, with velocity separations of 20, 120 and 0 km/s (see table 3). This may be interpreted as saying that the cross-section of galaxies with luminosities greater than 1/10 of L* for $\log(\mathrm{NH}) > 10^{13}$ is between 0.5 and 1 Mpc, although by "cross-section" we do not mean that the absorbers are neccessarily associated with the actual galaxy in question.

Because of the 3 Virgo absorbers, all of the Virgo galaxies have an absorber within 400 km/s. However, it is clearly unreasonable to suggest that more than one galaxy is associated with a given absorber. Thus of the 19 Virgo galaxies within 500 kpc of the line-of-sight, 16 must not be producing absorption. Of these 19, 2 have absolute magnitudes brighter than $1/10~\rm L^*$, and so are consistent with the above statement, despite the higher absorber EW limit, as long as only one of the galaxies with luminosity $<1/10~\rm L^*$ is producing observed absorption.

3.4.2. The Most Isolated Lyman α Absorbers

One of the stronger lines in our absorber sample is also the most isolated. Any galaxy brighter than -18 would be in our sample at the redshift of the isolated z=0.06655 absorber. However, the nearest such galaxy has a projected separation of 4.75 Mpc and a velocity difference of 710 km/s, which corresponds to a spatial separation of 10 Mpc for both pure and perturbed Hubble flow models. Indeed studying the galaxy distribution in figure 5, the three absorbers with 0.060 < z < 0.07 seem to lie in a 'void' in the galaxy distribution. While it is certainly possible that these absorbers are associated with galaxies below our absolute magnitude limit, these isolated absorbers are a clear demonstration that one can not associate ALL low-redshift Lyman α absorbers with luminous (L^*) galaxies.

3.4.3. The Absence of Lyman α Absorbers in the z ~ 0.078 Galaxy Concentration

The most striking feature of the observed galaxy redshift distribution is a concentration of galaxies cen-

tered at a redshift of $z \sim 0.078$. This excess is almost certainly associated with a structure which includes the galaxy cluster Abell 1564. This cluster has a tabulated center at 12:32:25 + 02:07:11 (1950), giving it an offset of 89' SW of the 3C273 sightline. This angle corresponds to a separation of 7.3 Mpc at the cluster distance. Abell 1564 is the closest Abell cluster to the 3C273 sightline, but is only richness class 0. Redshifts for two member galaxies are given in Metcalfe et al. 1989, giving an average cluster redshift of 0.0793. Selecting all galaxies in our fiber sample with redshifts between 0.07 and 0.085 (54 galaxies), one derives a mean redshift of 0.0781 with rms of 0.0021 (630 km/s). For comparison, selecting galaxies between redshifts of 0.15 and 0.17 (the cluster around 3C273, see figure 3), one gets 24 galaxies with mean redshift 0.1581 and rms 0.0024 (720 km/s).

Despite the location of Abell 1564 to the SW, the galaxies in the redshift slice 0.07-0.085 show a weak concentration to the NE of the fiber field, although there are galaxies in all parts of the fiber area surveyed. If they are really part of a structure including A1564, the structure must have a size of at least 8 Mpc. However, the nearest Lyman α absorber is 0.0095 from the peak in redshift space (or 2850 km/s, which is 4.5 times the rms from the mean of the concentration) and is at a distance of 36 Mpc from the center of the concentration. It thus seems unlikely that there are any observed Lyman α absorbers in our line of sight which are physically associated with this concentration.

We can test a slightly different form of the hypothesis considered in \S 3.3.4., (though we grant its application to the z \sim 0.078 galaxy concentration involves post facto statistics), namely: What is the probability that, if the Lyman α absorbers are distributed in space "in the same way" as the galaxies in our sample, we should find the observed number of Lyman α absorbers (none, in our case). By "in the same way" we mean that:

$$\left(\frac{\rho_{Ly\alpha}(\vec{r})}{\overline{\rho_{Ly\alpha}}}\right) = \left(\frac{\rho_{galaxy}(\vec{r})}{\overline{\rho_{galaxy}}}\right)$$

and by "in the vicinity of" we shall mean within $\pm 2.5 \times \mathrm{rms}$ of the redshift peak of the concentration. We consider that our selection function can be meaningfully applied over the redshift range from about z=0.016 out to our adopted "proximity cutoff" at z=0.151. Carrying out the integration of our sample (i.e. the galaxy numbers weighted by the selection

function) between $\pm 2.5 \times \mathrm{rms}$ of the peak of the galaxy concentration and over the redshift range from 0.016 to 0.151 we find that after correction for the selection function, about 0.33 of an absolute-magnitude-limited cylindrical sample of galaxies should be found within 2.5σ of the velocity peak of this structure. Since the Lyman α absorbers are not subject to such a selection function, we can apply this equation to all the volume elements along the line of sight and, assuming further that the effective cross-section of the Lyman α absorbers (σ) is constant over the redshift range 0.016-0.151, one can write:

$$n \times \sigma \times [(z_{peak} + 2.5 \times \text{rms}) - (z_{peak} - 2.5 \times \text{rms})]$$

= $0.33 \times \overline{n \times \sigma} \times [0.151 - 0.016]$

This equation represents the number of Lyman α absorbers in the vicinity of the peak that we should expect to see if our hypothesis is correct. Over the redshift interval 0.016-0.151 we have observed up to 14 Lyman α absorbers so that we expect $0.33 \times 14 \approx 4.7$ absorbers, and we observe none. The probability of this occuring is thus $exp(-4.7) \approx 0.01$. This is not a strong result due to the rather small number of absorbers expected, and the post facto nature of the test as we acknowledged above, but is additional suggestive evidence that the Lyman α absorbers do not follow the galaxy distribution and in particular that they may avoid strong concentrations of galaxies. It could be strengthened, of course, by observing additional lines of sight through dense concentrations.

It would be nice to repeat the above calculation for the case of the three absorbers found in the Virgo velocity region. However, there are a number of reasons why any estimate of the probability of finding three absorbers in this region with an apparent overdensity of galaxies is highly uncertain. Firstly, our absorber sample is incomplete in this velocity range, as described in § 3.3.1. Secondly, the area of sky surveyed is so small that the selection function correction for this velocity range is very large. Taking our selection function at face value, the 8 galaxies actually in our survey at Virgo velocities imply that 60% of an absolute-magnitude-limited cylindrical galaxy sample from z=0 to 0.151 would be found in that velocity range. Our hypothesis above would then predict that (neglecting the incompleteness of the absorber sample) one would expect $0.6 \times 17 \approx 10$ absorbers, when we only see 3. Unfortunately, it is not possible to place a meaningful uncertainty on this apparent under-density of absorbers in the Virgo region, for the reasons listed above.

In summary, there is marginal evidence, both from a clump of galaxies at z=0.078 and also from the Virgo velocity range, that Lyman α absorbers are less common in regions of high galaxy density.

4. Summary and Discussion

We have assembled several types of observations in an attempt to find objects with which the Lyman α absorbers along the line of sight to 3C273 might be associated, and in order to carry out statistical tests of galaxy-Lyman α absorber association. In particular, we obtained narrow-band images centered on and off the expected position of any $H\alpha$ emission which might be associated with three of the low redshift Lyman α absorbers, and obtained deep broad-band images of a 17'×17' field centered on 3C273. Both these searches were negative. Our failure to identify any broad-band or H α emission from plausible "galaxylike" objects a few tens of kpc from the 3C273 sight line at the approximate distance of the Virgo cluster will be checked by more sensitive and extensive searches for $H\alpha$ by T. Williams (private communication) and 21 cm emission by van Gorkom 1993 and van Gorkom et al. 1993.

We have also obtained redshifts for a large number of galaxies in the vicinity of the 3C273 sightline. Again, we find no unambiguous instance of association of any of the Lyman α absorbers with individual galaxies. We define a number of samples for both the Lyman α absorbers and the galaxies and estimate the 3-dimensional separation between each galaxy-galaxy pair and each Lyman α absorber-galaxy pair based upon two models for converting the observed redshift difference between any pair into a radial separation, viz. i) the assumption of a pure Hubble flow and ii) a statistical model of "perturbed" Hubble flow based upon work of Davis and Peebles 1983. The resulting data base is used to carry out statistical tests to confirm or reject two null hypotheses about the association of galaxies and Lyman α absorbers, namely: i) The Lyman α absorbers show no tendency to cluster around galaxies ii) The Lyman α absorbers cluster around galaxies exactly as the galaxies cluster about each other. While neither of these two hypotheses can be unambiguously rejected in the sense that every combination of samples and flow hypotheses reject both of them at significant levels, the evidence from

these tests, and from the galaxy-galaxy and Lyman α absorber-galaxy two-point correlations themselves, points quite strongly to the conclusion that both hypotheses are false.

In particular, over length scales from about 1 to 10 Mpc there seems little doubt that the Lyman α absorbers cluster around galaxies less strongly than the galaxies themselves cluster. This is born out by an examination of a redshift interval centered at about z=0.078 at which a strong concentration of galaxies occurs but in the neighborhood of which there are no Lyman α absorbers. Additionally, we find at least one Lyman α absorber for which no galaxy with absolute magnitude brighter than about -18 can be found closer than about 5 Mpc. Taken together, all this evidence suggests that the most significant conclusion we have reached is that the majority of low-redshift Lyman α absorbers are not intimately associated with normal luminous galaxies.

In view of the fact that it has long been realized that at high redshifts there is an absence of power in the Lyman α absorber two-point correlation function in redshift space, except possibly at the very smallest velocity separations, this conclusion is not too surprising. On the other hand, it is also fairly clear that there is *some* tendency for the Lyman α absorbers to cluster around galaxies, and even weak evidence that this clustering becomes strong at very small separations. Also Bahcall et~al.~1992a have investigated the auto-correlation function of the low-redshift absorbers seen in the line-of-sight to H1821+643, and show that there is only a 4% probability that the observed 'clumping' arose from a randomly distributed sample.

None of the foregoing points unambiguously, in our estimation, to a particular model for the formation and evolution of the Lyman α absorbers. As have others, we simply offer the following speculations which appear to be compatible with the facts as they are presently understood:

At high redshifts, the Lyman α absorbers consist primarily of entities which are only very loosely associated with larger mass objects (e.g. proto galaxies), and which are evolving fairly rapidly. Possibly this dominant population consists of absorbers in which gravitational binding (eg by dark matter) plays no significant role. In addition to this group, there is a smaller population of absorbers which are evolving less rapidly, possibly stabilized by dark matter and which are clustered more strongly about galaxies. At

very low redshifts, this latter population is beginning to constitute a large enough fraction of the absorbers that power in the two-point correlation function is detectable. Thus, the present mix of Lyman α absorbers appears to have clustering properties intermediate between present-epoch normal galaxies and a random non-clustered population. This property also appears to be shared by the low-luminosity moderate redshift "blue galaxies" (Pritchet and Infante 1992), leading to the plausible conjecture that the Lyman α absorbers are more closely related to low mass, low luminosity galaxies than they are to L* galaxies, though the relation is clearly not one-to-one.

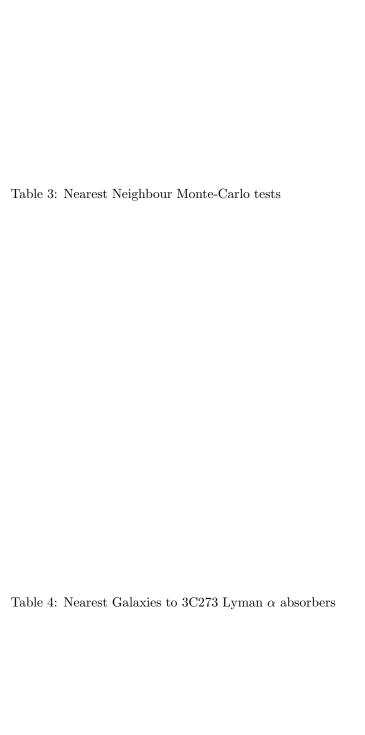
We have no good way at present of estimating the characteristic scale or masses of the low-redshift Lyman α absorbers. A guess at a diameter of 30 kpc is as plausible as any. In particular, consider a pancake whose diameter is 30 kpc and whose thickness is 10 kpc. In this case, at the present epoch, a hydrogen column-density of 10^{13} - 10^{14} cm⁻² normal to the face of the absorber, coupled with estimates for the present-epoch energy-density of ionizating radiation leads to a total gas mass of order $10^7 M_{\odot}$, but a mass of only a few hundred solar masses of neutral hydrogen. It is of interest that the mass function of neutralhydrogen gas clouds appears to be truncated below about $10^8 \,\mathrm{M}_{\odot}$ (Weinberg et al. 1991). As Maloney (1992,1993) has shown, the gas in a flaring galaxy with decreasing column-density will undergo a rather sudden transition along its face from being mostly neutral to mostly ionized, with the consequence that few if any contours with neutral-hydrogen columndensity of order 10^{18} cm⁻² are known. Similarly, it is conceivable that, given the appropriate run of length scale with mass, a sequence of masses would have the property of making a sudden transition in the mass function of neutral-hydrogen starting at about 10^8 M_{\odot} , leading to a dearth of objects with total HI masses for several orders of magnitude below this.

If these speculations have any connection with reality then one might expect to see some similarity in the clustering properties of the Lyman α absorbers and low mass galaxies. We are currently attempting to obtain redshifts of galaxies of lower luminosity along the 3C273 sightline in order to investigate this possibility.

We would like to thank Greg Aldring and Steve Shectman for help and advice in using the LCO fiber system, Neil Reid for giving us access to one of the new Palomar Sky-survey plates, Alan Sandage for allowing us to inspect one of his older IIIaJ plates, Mark Davis and Margaret Geller for advice on generating Monte Carlo samples with known correlation functions, Don Schneider for help with the JASON software and Xavier Barcons, Donald Lynden-Bell, Mario Mateo, Houjon Mo, Michael Rauch, John Webb, Jeff Willick and Dennis Zaritzky for useful conversations. We would also like to thank the referee, J. N. Bahcall, for his helpful and constructive comments which improved the content and presentation of the paper. SLM and RJW acknowledge support through NASA contract NAS5-30101 and NSF grant AST-9005117.

Table 1: Definite Galaxy redshifts in 3C273 Field

Table 2: Comparison of 3C273 Extragalactic Absorption Line Lists



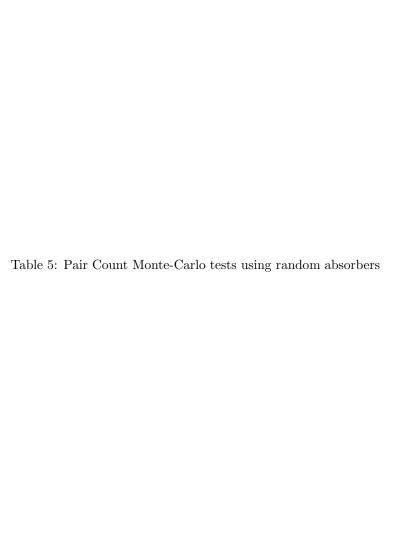


Table 6: KS comparison of z-distribution

Table 7: Pair Count Monte-Carlo tests using the galaxy distribution

REFERENCES

- Allen, C. W. 1973, "Astrophysical Quantities 3rd Edition", Athlone Press, London, Pg 267
- Bahcall, J. N., Jannuzi, B. T., Schneider, D. P., Hartig, G. F., Bohlin, R. and Junkkarinen, V., 1991a, in "The First Year of HST Observations", ed A. L. Kinney and J. C. Blades, Pg 46
- Bahcall, J. N., Jannuzi, B. T., Schneider, D. P., Hartig, G. F., Bohlin, R. and Junkkarinen, V., 1991b, ApJ, 377, L5
- Bahcall, J. N., Jannuzi, B. T., Schneider, D. P., Hartig, G. F. and Green, R. F., 1992a, ApJ, 397, 68
- Bahcall, J. N., Jannuzi, B. T., Schneider, D. P., Hartig, G. F. and Jenkins, E. B., 1992b, ApJ, 398, 495
- Bahcall, J. N., Bergeron, J., Boksenberg, A., Hartig,
 G. F., Jannuzi, B. T., Kirhakos, S., Sargent, W.
 L. W., Savage, B. D., Schneider, D. P., Turnshek,
 D. A., Weymann, R. J. and Wolfe, A. M., 1993,
 ApJS, In Press
- Binggeli, B., Sandage, A. and Tammann, G. A., 1985, AJ, 90, 1681
- Brandt, J. C. et al., 1993, AJ, 105, 831
- Chernomordic, V. V. and Ozernoy, L. L., 1983, Nature, 303, 153
- Davis, M. and Peebles, P. J. E. 1983, ApJ, 267, 465
- Fransson, C. and Epstein, R., 1982, MNRAS, 198, 1127
- Haynes, M.P. and Giovanelli, R. 1984, AJ, 89, 758
- Huchra, J. P. 1990 May 5 1990 version of the CfA Redshift Catalog, obtained through the Astronomical Data Center.
- Jacoby, G. H., Branch, D., Ciardullo, R., Davies, R. L., Harris, W. E., Pierce, M. J., Pritchet, C. T., Tonry, J. L. and Welch, D. L., 1992, PASP, 104, 599
- Kennicutt, R. C., 1984, ApJ, 287, 116
- Kent, S. M., 1985, PASP, 97, 165
- Loveday, J., Peterson, B. A., Efstathiou, G. and Maddox, S. J., 1992, ApJ, 390, 338

- Maloney, P., 1992, ApJ, 389, L89
- Maloney, P., 1993, ApJ, In Press
- Massey, P., 1990, NOAO Newsletter # 21, March 1990
- Mo, H. J., Jing, Y. P. and Borner, G., 1992, ApJ, 392, 452
- Mo, H. J., Einasto, M., Xia, X. Y. and Deng, Z. G., 1992, MNRAS, 255, 382
- Mo, H. J., Morris, S. L. and Weymann, R. J., In Preparation
- Metcalfe, N., Fong, R., Shanks, T. and Kilkenny, D. 1989, MNRAS, 236, 207
- Morris, S. L., Weymann, R. J., Savage, B. D. and Gilliland, R. L., 1991, ApJ, 377, L21
- Osterbrock, D. E., "Astrophysics of Gaseous Nebulae and Active Galactic Nuclei", 1989, University Science Books, CA
- Phillips, S., Disney, M. J. and Davies, J. I., 1993, MNRAS, 260, 453
- Pritchet, C. J. and Infante, L., 1992, ApJ, 399, L35
- Rauch, M, Carswell, R. F., Chaffee, F. H., Foltz, C. B., Webb, J. K., Weymann, R. J., Bechtold, J. and Green, R. F., 1992, ApJ, 390, 387
- Salzer, J. J. 1992, AJ, 103, 385
- Sandage, A. and Bingelli, B., 1984, AJ, 89, 919
- Savage, B. D., Lu, L., Weymann, R. J, Morris, S. L. and Gilliland, R. L., 1993, ApJ, 404, 124
- Schneider, D. P., Hartig, G. F., Jannuzi, B. T.,
 Kirhakos, S., Saxe, D. H., Weymann, R. J., Bahcall, J. N., Bergeron, J., Boksenberg, A., Sargent,
 W. L. W., Savage, B. D., Turnshek, D. A. and
 Wolfe, A. M., 1993, ApJS, In Press
- Shectman, S. A., 1992, in "Fiber Optics in Astronomy II", ed P. M. Gray, ASP Volume 37, Pg 26
- Songaila, A., Bryant, W. and Cowie, L. L., 1989, ApJ, 345, L71
- Stockton, A. 1980, In IAU symposium 92, "Objects of High Redshift", ed G. O. Abell and P. J. E. Peebles, Pg 87

- van Gorkom, J., H., 1993, Teton Conference Proceedings, In Press, Ed M. Shull and H. Thronson
- van Gorkom, J., H., Bahcall, J.N., Jannuzi, B., and Schneider.D. 1993, AJ, In Press
- Vilas, F. and Smith, B. A., 1987, Appl.Optics, 26, 4
- Weinberg, D. H., Szomoru, A., Guhathakurta, P. and van Gorkom, J. H., 1991, ApJ, 372, L13

This 2-column preprint was prepared with the AAS LATEX macros v3.0.

Fig. 1.— Coronagraph Data of 3C273 field. (a) Sum of 25Å Filters, the horizontal bar in the lower left is 1 armin long, (b) Continuum Subtracted VN1, (c) Continuum Subtracted VN2, (d) Continuum Subtracted HN. See text in § 2.1.

Fig. 2.— Mosaic of COSMIC Images in Gunn r of 3C273 field. See text in \S 2.2. Region shown in figure 1 is circled.

Fig. 3.— Histogram of redshifts for Galaxies found in the 3C273 sightline. Also plotted are the locations of Lyman α absorbers from table 3 (where 'strong' refers to lines with EW \geq 55 mÅ, and 'weak' refers to the remainder), and the (arbitrarily normalised) galaxy selection function for the fiber survey. See text in § 2.3.

Fig. 4.— Locations on the sky of the galaxies with redshifts in the field of 3C273. See text in § 2.3.

Fig. 5.— Pie-diagrams for the Galaxies observed with the LCO fiber system. Angles have been exagerated by a factor 15 to prevent overcrowding of the symbols. Please note that this results in a highly distorted plot with initially spherical structures (such as the 3C273 cluster of galaxies) appearing elongated transverse to the line of sight. Note also that the star marking the position of 3C273, while readily visible in the projection in RA, is partially obscured by a clump of galaxies in the projection in Dec

Fig. 6.— Mosaic of COSMIC Images in Gunn r of 3C273 field, with 3 artificial dwarf galaxies added. NE with $\rm M_B{=}{-}14.5$ and scale length 15kpc, NW with $\rm M_B{=}{-}13.5$ and scale length 7.5kpc, and SW with $\rm M_B{=}{-}13.5$ and scale length 15kpc. See text in \S 3.2.

Fig. 7.— Two point correlation functions for galaxy-galaxy and absorber-galaxy (a) assuming pure Hubble flow (b) assuming perturbed Hubble flow. See text in § 3.3.4.

This figure "fig1-1.png" is available in "png" format from:

This figure "fig1-2.png" is available in "png" format from:

This figure "fig1-3.png" is available in "png" format from:

This figure "fig1-4.png" is available in "png" format from:

This figure "fig1-5.png" is available in "png" format from:

This figure "fig1-6.png" is available in "png" format from:

This figure "fig1-7.png" is available in "png" format from: